# FLUIDIC-BASED VIRTUAL AEROSURFACE SHAPING

**Ari Glezer**
**Woodruff School of Mechanical Engineering**
**Georgia Institute of Technology**

## Abstract

Recent work on a novel approach to the control of the aerodynamic performance of lifting surfaces by *fluidic modification of their apparent aerodynamic shape, or virtual aerosurface shaping* is reviewed. This flow control approach emphasizes fluidic modification of the "apparent" aerodynamic shape of the surface with the objective of altering or prescribing the streamwise pressure gradient. Control is effected by the interactions of arrays of synthetic jet actuators with the cross flow that displace the local streamlines near the surface and thereby induces an 'apparent' modification of the flow boundary. The operating frequency of the control jets is high enough so that the actuation period is at least an order of magnitude *lower* than the relevant characteristic time scale of the flow. Therefore, the interaction domains between the control jets and the cross flow are quasi-steady and hence the induced aerodynamic forces are virtually time-invariant.

These effects are investigated at two practical domains of the flight envelope. The first is at post stall angles of attack where the ability to suppress separation implies robust control over large changes in circulation and accumulation and shedding of vorticity. An important element of this approach is the evolution and coherence of the vertical structures within the controlled wake with the objective of mitigating unsteady aerodynamic forces. The second domain is that of small angles of attack when the baseline flow is typically fully attached and therefore less amenable to flow control approaches that require separation.

## I. Overview

Flow control strategies for external aerodynamic surfaces have mostly focused on mitigation of flow separation which is typically precipitated by an adverse pressure gradient (e.g., on a lifting surface) or by a sharp discontinuity in the flow boundary (e.g., a cavity or a bluff trailing edge). Attempts to manipulate and ultimately control separation over stalled airfoils (and other bluff bodies) have typically relied on the narrow band receptivity of the separating flow to external actuation. The separation is simultaneously affected by *two* instability mechanisms namely, a local instability of the separating shear layer and, more importantly, an instability of the wake that ultimately results the formation and shedding of large-scale vortical structures into the wake (e.g., Wu et al., 1998). Because the nominally time-periodic vortex shedding into the wake is accompanied by global changes in circulation, it strongly affects the evolution of the separating shear layer downstream of the leading edge. In fact, this coupling appears to dominate the rollup of the shear layer whose natural ("most unstable) frequency is typically higher than the global shedding frequency.

Since the characteristic scale of the wake is typically commensurate with the scale of the separated flow domain, earlier work on separation control over fully- or partially-stalled airfoils has emphasized actuation frequencies that are on the order of the shedding frequency. This corresponds to a Strouhal number $St_{act} = (L/U_c)/T$ that is O(1) where the actuation period $T$ is

*Paper presented at the RTO AVT Specialists' Meeting on "Enhancement of NATO Military Flight Vehicle Performance by Management of Interacting Boundary Layer Transition and Separation", held in Prague, Czech Republic, 4-7 October 2004, and published in RTO-MP-AVT-111.*

# Report Documentation Page

*Form Approved*
*OMB No. 0704-0188*



| 1. REPORT DATE | 2. REPORT TYPE | 3. DATES COVERED |
|---|---|---|
| **01 OCT 2004** | **N/A** | **-** |

| 4. TITLE AND SUBTITLE | 5a. CONTRACT NUMBER |
|---|---|
| **Fluidic-Based Virtual Aerosurface Shaping** | 5b. GRANT NUMBER |
| | 5c. PROGRAM ELEMENT NUMBER |
| 6. AUTHOR(S) | 5d. PROJECT NUMBER |
| | 5e. TASK NUMBER |
| | 5f. WORK UNIT NUMBER |
| 7. PERFORMING ORGANIZATION NAME(S) AND ADDRESS(ES) **Woodruff School of Mechanical Engineering Georgia Institute of Technology** | 8. PERFORMING ORGANIZATION REPORT NUMBER |
| 9. SPONSORING/MONITORING AGENCY NAME(S) AND ADDRESS(ES) | 10. SPONSOR/MONITOR'S ACRONYM(S) |
| | 11. SPONSOR/MONITOR'S REPORT NUMBER(S) |

12. DISTRIBUTION/AVAILABILITY STATEMENT
**Approved for public release, distribution unlimited**

13. SUPPLEMENTARY NOTES
**See also ADM201868, RTO-MP-AVT-111 Enhancement of NATO Military Flight Vehicle Performance by Management of Interacting Boundary Layer Tranisition and Separation (L'amelioration des performances des vehicules aeriens militaires de l'OTAN par la gestion de l'interaction entre la transition et le decollement de la couche limite)., The original document contains color images.**

14. ABSTRACT

15. SUBJECT TERMS

| 16. SECURITY CLASSIFICATION OF: | | | 17. LIMITATION OF ABSTRACT | 18. NUMBER OF PAGES | 19a. NAME OF RESPONSIBLE PERSON |
|---|---|---|---|---|---|
| a. REPORT | b. ABSTRACT | c. THIS PAGE | | | |
| **unclassified** | **unclassified** | **unclassified** | **UU** | **20** | |

comparable to the time of flight over the separated flow domain ($L$ and $U_c$ are the characteristic advection length and speed, respectively). This approach to control of separation has been applied with varying degrees of success since the early 1980s to restore aerodynamic performance of stalled airfoils and flaps (e.g., Ahuja and Burrin, 1985, Hsiao et al., 1990, Neuburger and Wygnanski, 1987, and Seifert et al., 1993). Seifert et al. (1984) argued that the actuation is most effective when the "reduced frequency" $F^+$ (which is essentially the Strouhal number $St_{act}$) is of order 1 indicating that *the actuation frequency couples to, and in fact drives the shedding* in the near wake. Actuation at these frequencies leads to the formation of vortical structures that scale with the length of the separated flow domain and the ensuing changes in the rate of entrainment result in a Coanda-like deflection of the separating shear layer towards the surface of the stalled airfoil such that the layer vortices are effectively advected downstream in close proximity to the surface (e.g., Amitay and Glezer 2003). The coupling (or feedback) between (nominally) time-periodic shedding of coherent vortices and the separated shear layer becomes more pronounced in the presence of actuation and can intensify the unsteady component of the global aerodynamic forces. Some of these unsteady effects were discussed in the earlier works of Amitay and Glezer (1999, 2002) and are also evident in the numerical simulations of Wu et al. (1998).

A different approach to the control of flow separation on lifting surfaces emphasizes fluidic modification of the "apparent" aerodynamic shape of the surface upstream of separation with the objective of altering the streamwise pressure gradient to achieve complete or partial bypass (or suppression) of separation. Actuation is effected by forming a controlled interaction domain between a surface-mounted fluidic actuator (e.g., a synthetic jet, Smith and Glezer, 1988) and the cross flow above the surface. As demonstrated by Honohan et al. (2000) and Honohan (2003) on a two-dimensional cylinder, the interaction domain between a high-frequency synthetic jet and the cross flow over the surface displaces the local streamlines of the cross flow and thereby induces a 'virtual' change in the shape of the surface (measuring roughly 2-4 actuation wavelengths). The resulting change in the streamwise pressure gradient alters the evolution of the boundary layer and leads to a delay in separation. In connection with these findings, it is noteworthy that the formation of a small, closed separation bubble on the surface of a cylinder (at $Re_D \approx 3.2 \cdot 10^5$) *in the absence of flow actuation* allows the boundary layer to withstand higher than normal pressure rise and thus *flow separation moves farther downstream* and the cylinder base pressure increases (Roshko and Fiszdon, 1969). The modification of the apparent shape of aerodynamic surfaces has been exploited for controlling the evolution of both wall-bounded and free shear flows (e.g., stalled airfoils, Amitay et al., 1998, and jet vectoring, Smith and Glezer, 2002, respectively). Because active modification of the apparent shape of aerodynamic surfaces can potentially enable the tailoring of the pressure gradient on existing surfaces to overcome adverse pressure gradient and local separation, it may enable unconventional aerodynamic design approaches that are driven primarily by mission constraints (e.g., payload, stealth, volume, etc.). The compromised aerodynamic performance of such designs could potentially be augmented by the use of apparent surface modification to maintain aerodynamic performance throughout the flight envelope (e.g., Kondor et al.,2001 and Fung and Amitay, 2002).

In contrast to separation control approaches that rely on global manipulation of the coupled shear layer/wake instabilities (where the characteristic actuation period scales with the advection time of the affected flow domain) "virtual" surface shaping is based on actuation having a characteristic wavelength that is at least an order of magnitude smaller than the relevant local or global length scales of the flow. Therefore, the corresponding actuation frequencies for these

two approaches are at least an order of magnitude apart, namely on the order of and about ten times larger than the shedding frequency, respectively. In fact, "virtual" surface shaping emphasizes an actuation frequency that is high enough so that the interaction between the actuator and the cross flow is essentially time-invariant on the global time scale of the flow (e.g., vorticity shedding) and therefore is effectively frequency independent. The effectiveness of high actuation frequency has been demonstrated in several previous works on separation control including Amitay et al (1999, $10 < St_{act} < 20$) Erk (1997, $St_{act} \approx 100$) and more recently Pack Melton et al. (2004, $St_{act} = 15$). Amitay and Glezer (2002) demonstrated that since high actuation frequencies are effectively decoupled from the wake instability, the derived aerodynamic forces tend to be virtually time-invariant.

Besides the effectiveness of this actuation approach for separation control, recent work at Georgia Tech (Chatlynne et al., 2001 and Amitay et al., 2001) has demonstrated the utility of high frequency aerosurface modification for aerodynamic flow control even in the absence of stall which is of particular interest for cruise conditions at low angles of attack. Significant reduction in form drag with minimal lift penalty was achieved on a Clark-Y airfoil by the formation of a trapped vortex the interaction domain between a synthetic jet and a miniature (nominally $0.01c$) surface-mounted passive obstruction downstream of the leading edge of a conventional airfoil. More recently, DeSalvo et al. (2002) improved the performance of a NACA 4415 airfoil using a small trailing edge obstruction that is similar to a Gurney flap (e.g., Liebeck, 1978, Jeffrey et al., 2000) on the pressure surface and manipulated the trapped vortex behind it using an integral synthetic jet actuator to realize a 15% improvement in $L/D$ compared to the baseline configuration. Control of the trapped vorticity downstream of the flap alters the Kutta condition and results in modification of the aerodynamic performance of the airfoil at low (cruise) angles of attack *without moving control surfaces*.

The present paper reviews recent work on the effects of changes in the apparent aerodynamic shape of a lifting surface at two practical limits of the flight envelope. The first is at post-stall angles of attack where the ability to suppress separation implies robust control over large changes in circulation and accumulation and shedding of vorticity both for quasi-steady (§II) and transient, time-modulated (§IV) actuation inputs. While the former leads to virtually time-invariant aerodynamic forces, the latter exploits transient response of the flow to increase the aerodynamic forces and moments. The second limit is that of small angles of attack when the baseline flow is typically fully attached and therefore less amenable to flow control approaches that address stall (§V). The structure and evolution of virtual aerosurfaces that are induced by fluidic actuation is discussed in §III.

## II. Separation Control of a Stalled Airfoil

Conventional approaches for separation control have relied on the coupling between the instabilities of the wake and the separating shear layer global manipulation of the instability of the separating shear layer have been investigated since the early 1980's (e.g., Ahuja and Burrin, 1985). Similar, and in some cases even improved aerodynamic performance of stalled airfoils and bluff bodies has been demonstrated by fluidic modification of the "apparent" aerodynamic shape of the surface upstream of separation with the objective of altering the streamwise pressure gradient to achieve complete or partial bypass (or suppression) of separation. The actuation is effected by forming a controlled interaction domain between a surface-mounted fluidic actuator (e.g., a synthetic jet) and the cross flow above the surface such that the resulting change in the streamwise pressure gradient alters the evolution of the boundary layer and can lead to

suppression or streamwise delay of separation. This has been typically accomplished using actuation effected by synthetic jet actuators, which were deliberately operated at frequencies that were at least *an order of magnitude higher* than the characteristic frequencies of the separating flow or of the near wake were reported by Chang et al., 1992, Erk, 1997, Smith et al., 1998 and Amitay et al., 2001 and more recently by Pack Melton et al (2004). However, as shown by Amitay and Glezer (1999, 2002), although the restored time-averaged aerodynamic forces that are attained by either control approach are nominally similar, low frequency actuation yields instantaneous forces that have a substantial time-dependent component (see also Wu et al 1998) while the corresponding forces at high actuation frequencies are essentially time-invariant.

The effects of the actuation frequency on the structure of the flow over a stalled, unconventional airfoil were discussed in the earlier work of Amitay and Glezer (2002). A sequence of phase-averaged smoke visualization images is shown in Figures 1a-f (the separated flow in the absence of actuation is shown for reference in Figure 1a). The smoke is injected in a sheet at center span and is illuminated at a given phase relative to the actuation signal using a Yag laser. In these experiments, $Re_C = 310{,}000$, the angle of attack is $\alpha = 15^o$, the jets angle with respect to the oncoming flow is $\gamma = 60^o$ and their combined momentum coefficient (the two jets are driven in phase) is $C_\mu = 1.8 \cdot 10^{-3}$. ($C_\mu = \bar{I}_j / \frac{1}{2}\rho_o U_o^2 c$, where $\bar{I}_j$ during the outstroke is $\bar{I}_j = \frac{2}{T}\rho_j b \int_0^{T/2} u_j^2(t)dt$, $T$ is the actuation period $\rho_j$ and $\rho_o$ are the jet and free-stream fluid densities, respectively, b is the jet orifice width, $c$ is the chord, and $U_o$ is the free-stream velocity, the jet speed at the exit plane $u_j$ is measured using a miniature hot-wire sensor.)

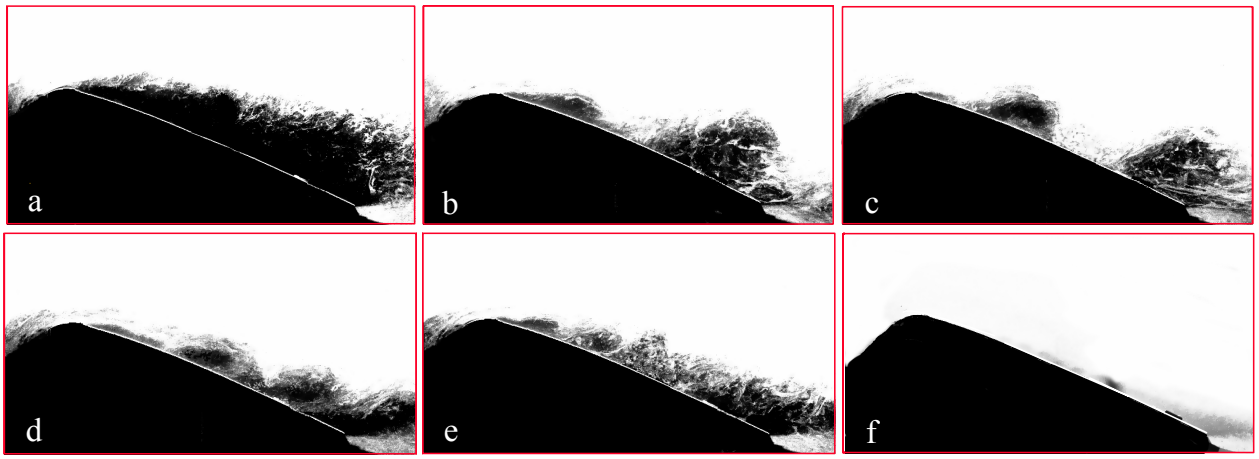


***Figure 1*** *Phase averaged smoke visualization images of the flow above the surface of the airfoil ($\alpha = 15^0$, $\gamma = 60^o$). Baseline (a), $St_{Cact} = 0.7$ (b), 1.1 (c), 2.05 (d), 3.3 (e), and 10 (f).*

For "low" $St_{act}$ [i.e., O(1), Figures 1b-d], the separated shear layer is deflected towards the surface and the passage frequency of the layer vortices is commensurate with $f_{act}$. These vortices persist well beyond the trailing edge of the airfoil, and is evident that because their formation frequency couples with the airfoil's natural shedding frequency ($St_{shed} = 0.7$), they are actually enhanced as they are advected downstream (as might be predicted by stability theory). When $St_{Cact}$ is increased to 3.3 (Figure 1e), the shear layer vortices become smaller and are somewhat smeared within the domain $0.5c$ and $0.7c$ (indicating some loss of phase locking to the actuation frequency), and the flow over the surface appears to be separated beyond $0.7c$. Although the stability of the separated shear layer was not analyzed, the loss of coherence and ultimate

separation in Figure 1e suggests that as the actuation frequency increases, the actuation becomes less effective. This would indicate that the actuation frequency (which is over four times the "natural" shedding frequency, $St_{shed} = 0.7$) is close to the upper end of the coupled receptivity band of the wake and the separating shear layer (cf. §I) and therefore is not significantly amplified.

Finally, when the actuation frequency is increased to $St_{Cact} = 10$ (Figure 1f), the flow appears to be fully attached to the top surface of the airfoil and there is no evidence of organized, phase-coherent vorticity concentrations. This indicates that when the actuation frequency is high enough, the flow upstream of the stalled domain is altered such that separation is bypassed and effectively suppressed. As discussed in connection with Figure 2, the suppression of separation at "high" $St_{act}$ results in reduction in the width of the wake and therefore decoupling of the actuation from the wake instability.

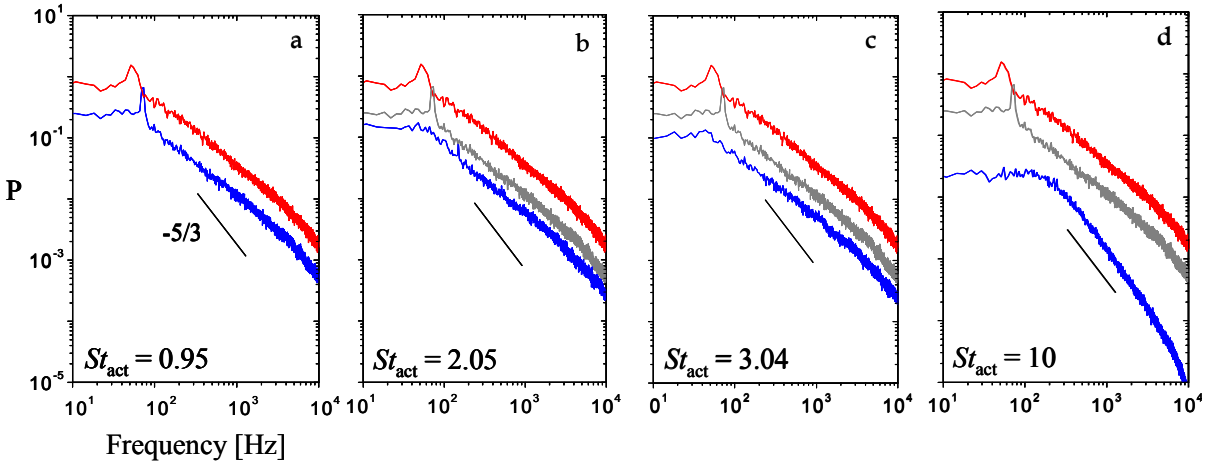


***Figure 2*** *Power spectra of the streamwise velocity in the wake of the airfoil: $St_{Cact} = 0.95$ (a), 2.05 (b), 3.3 (c), and 10 (d). The spectra in the absence of actuation and for $St_{Cact} = 0.95$ are repeated in each frame.*

The work of Amitay and Glezer (2002) showed that in the presence of actuation when the flow is nominally attached to the upper surface of the airfoil, the cross-stream extent of the wake is substantially reduced and is accompanied by a reduction in the magnitudes of rms velocity fluctuations within the wake. Spectra of the streamwise velocity within the wake (Amitay and Glezer, 2002) are reproduced in Figures 2a-d for the purpose of the present discussion. These power spectra are measured at $x/c = 2$ near the upper edge of the wake at a cross-stream elevation where the streamwise velocity deficit is half the maximum deficit. At $St_{Cact} = 0.95$ (Figure 2a) there is a strong spectral component at the actuation frequency and the entire spectrum appears to be attenuated by approximately 3.5. As $St_{Cact}$ is increased to 2.05 and 3.3, the spectral peak at the actuation frequency shifts towards the decaying part of the spectrum. Note that at $St_{Cact} = 3.3$, the spectral peak at the actuation frequency within the wake is virtually indistinguishable from the background indicating that even though the separated flow domain still exhibits discrete vortices at the actuation frequency, the wake is apparently not receptive to this frequency and therefore the coupling between the separating shear layer and the wake is diminished (cf. §I) and this spectral component decays. The reduction in the cross stream extent of the separated flow domain results in nearly uniform attenuation of all spectral components by 4.5 ($St_{Cact} = 2$) and 7 ($St_{Cact} = 3.3$).

When the actuation frequency is increased to $St_{Cact} = 10$ (Figure 2d), the resulting spectra are remarkably different from the corresponding spectra at the lower actuation frequencies. There is a considerably stronger attenuation (well over an order of magnitude) at both the low and high spectral ends, and the spectrum includes a distinct inertial sub-range for $St_C > 3$ over almost two decades *that also includes the actuation frequency*. The reduced power at all spectral components (compared to actuation at lower $St_{Cact}$) indicates that the absence of time-periodic vortex shedding into the wake and the diminished coupling to the wake instabilities at the higher actuation frequency results in lower energy transfer from the uniform stream. It is noteworthy that compared to $St_{Cact} = 0.95$, the high actuation frequency yields somewhat lower drag (7%) and higher lift (15%). As was shown by Wiltse and Glezer (1998), direct actuation at wave numbers that correspond to small-scales within the base flow can lead to increased dissipation and rapid transfer of energy from the large scales to the small scales Increased dissipation at high actuation frequencies that are within the spectral dissipation range of the wake.

The control effectiveness of the actuation in Figure 3 is measured by the variation of the ratio of lift to (pressure) drag $L/D_p$, with actuation frequency $St_{Cact} = 0.95$, 2.05, 3.4, 10, 14.7 and 20 (Figure 3). Two distinct domains are immediately apparent. In the first domain (I), where the actuation frequencies are of the same order as the shedding frequency ($St_{Cact} < 4$), $L/D_p$ decreases with increasing St (from 2.65 for $St_{Cact} = 0.95$ to 2.35 for $St_{Cact} = 3.3$), which may be the result of reduced receptivity of the separated shear layer. In the second domain ($St_{Cact} > 10$), the actuation frequency is at least an order of magnitude higher than the shedding frequency and the lift to pressure drag ratio is higher ($L/D_p \approx 3.2$). In fact, it appears that $L/D_p$ is almost independent of the actuation frequency, suggesting that the mechanism that leads to the suppression of separation is not associated with the stability of the separated shear layer. Unfortunately, bandwidth limitations of the low- and high-frequency actuators prevented overlap within the domain $4 < St_{Cact} < 10$.

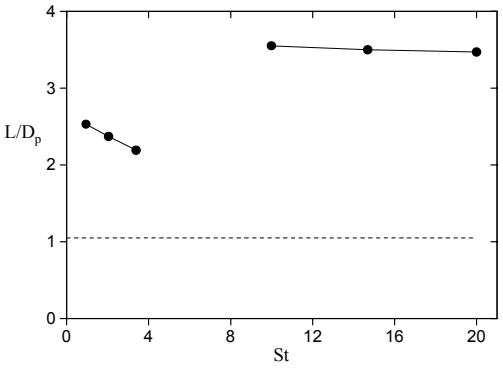


***Figure 3*** *Variation of $L/D_p$ with Strouhal number, $\gamma = 60^o$, baseline (---).*

## III Virtual Aerosurface Shaping

### *III.1 Some Features of the Interaction Domain between a Jet and a Cross Flow*

Although the interest in control of separation for aerodynamic applications has been primarily focused on 2-D and 3-D airfoils, some control strategies have been investigated in the nominally two-dimensional flow around circular cylinders (e.g., Williams et al., 1991 and Pal & Sinha, 1997). This simple geometry is particularly attractive since it minimizes higher-order effects of a *specific* global (e.g., airfoil) geometry and has the distinct advantage that the baseline flow is extensively documented including the evolution with Reynolds number of flow separation (e.g., Roshko and Fiszdon, 1969). Amitay et al. (1997 and 1998) investigated the effect of a surface mounted synthetic jet at $Re_D$ up to 130,000 over a range of jet angles and showed that the jets can effect an increase in lift of up to $C_L = 1$ and a corresponding reduction in pressure drag of up to 30%. The structure of the interaction domain between a jet and the nominally two-dimensional cross flow around the cylinder were investigated in detail (Honohan et al., 2000, Honohan, 2003, Glezer et al., 2004). High-resolution (0.133 mm) digital particle image velocimetry (PIV) was

used to investigate the nominally two-dimensional (time- and phase-averaged) flow field in the absence and presence of actuation within a domain that includes the synthetic jet actuator and the separating shear layer on the top surface of the cylinder. These measurements were conducted in a two-dimensional (0.91 x 0.051 m cross section), closed return wind tunnel using a 63 mm cylinder model equipped with a 2-D jet actuator having an orifice width of 0.5 mm. The cylinder can be rotated about its centerline so that the angle between the jets and the direction of the free stream can be continuously varied.

The interaction domain between the jet and the cross flow at high actuation frequency is inferred from distributions of the spanwise vorticity (Figures 4a-c) that are measured along the surface of the cylinder at $Re_D = 21{,}500$ (to provide a thicker boundary layer). The time-averaged vorticity map in Figure 4a shows that the baseline flow separates at $\theta \approx 90^o$. Phase-averaged vorticity concentrations in the presence of actuation (Figure 4b) show that the (counter rotating) vortex pairs that engender the jet interact with the wall boundary layer and form a train of clockwise (CW) vortices that are advected downstream, become weaker and ultimately disappear within three to four wavelengths of the actuation ($\lambda = 0.5U_\infty/f_{act}$). These data also show that the (upstream) counterclockwise (CCW) jet vortex is accelerated above and around the CW vortex and rapidly weakens (within one wavelength). The time-averaged vorticity in the presence of actuation (Figure 4c) shows a *finite* interaction domain that protrudes into the cross flow above the edge of the local boundary layer in the absence of actuation and ends approximately 2-3$\lambda$ downstream from the jet orifice and is followed by a *thinner boundary layer compared to the baseline flow*.

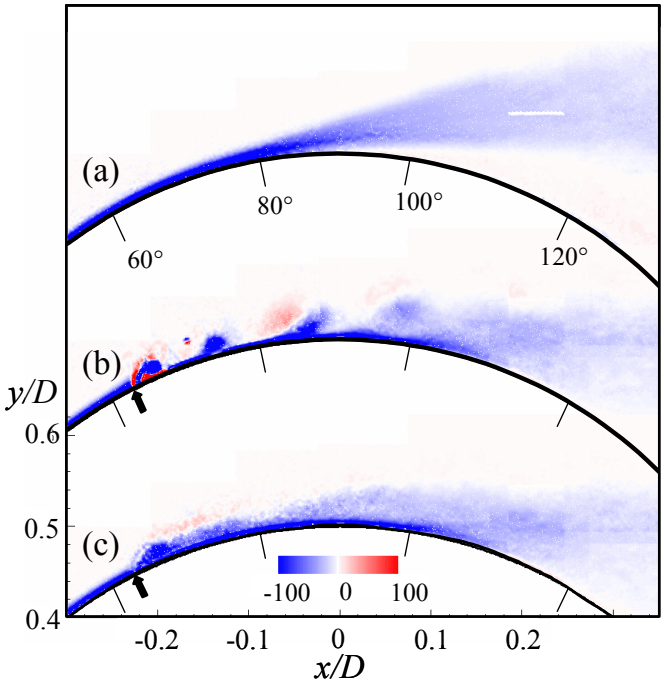


***Figure 4*** *Normalized vorticity $St_{Dact}$ = 4.0 baseline (a), and actuated: phase-locked (b), and time-averaged (c). ($\gamma = 63^0$, $C_\mu = 5.1x10^{-2}$).*

The interaction domain in Figure 4c displaces the outer flow and thereby results in local variations in the time-averaged pressure field, which is computed from the Reynolds-averaged Navier-Stokes equations using the PIV data. Figure 5a shows two streamlines having the same value of the stream function in the absence and presence of actuation that are superposed on the vorticity distribution of the actuated flow (note the displacement of the streamline in the presence of the actuation). Here, b is the jet's orifice width. The corresponding pressure distributions along these streamlines are shown in Figure 5b. Compared to the baseline flow, the pressure along the streamline in the presence of actuation is lower over the entire measurement domain, indicating an increase in the velocity along the streamline due to global changes in the flow (e.g., the movement of the separation point). More significantly, within the azimuthal sector that includes the interaction domain there is a local minimum in the pressure distribution that indicates a significant favorable pressure gradient in the cross flow above the interaction domain.

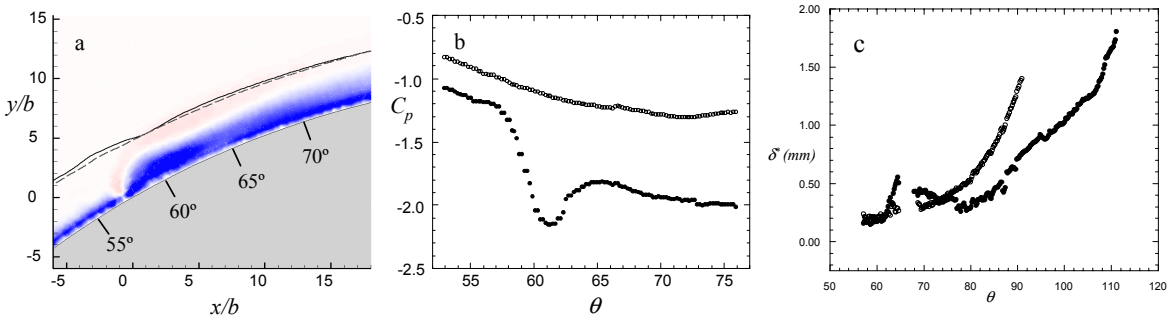


***Figure 5.*** *(a) Vorticity in interaction domain superimposed with streamlines having the same stream function value: baseline (-----) and actuated (———); The pressure coefficient along the streamlines (b) and the boundary layer displacement thickness (c): baseline (○), actuated (●).*

The favorable gradient is followed by a small region of weaker adverse pressure gradient, and finally, there is a slight favorable pressure gradient through the rest of the domain. As can be inferred from Figure 5c, the alteration of the streamwise pressure gradient results in a thinner, more stable, boundary layer downstream of the interaction domain and a substantial delay in separation. The evolution of the (time-averaged) boundary layer displacement thickness $\delta^*$ for the baseline and actuated flows are shown in Figure 5c. Within the interaction domain, ($60° < \theta < 80°$), $\delta^*$ in the presence of actuation increases, reaches a local maximum immediately downstream of the jet, and then diminishes substantially suggesting the presence of a favorable streamwise pressure gradient. For $\theta > 80°$, $\delta^*$ begins to increase again although at a lower streamwise rate than in the absence of actuation, until separation occurs at $\theta = 110°$.

### *III.2 Aerosurface Modification:The Drag Crisis and Transition to Turbulence*

Perhaps one of the most striking features of the flow about a circular cylinder is the occurrence of the "drag crisis" as the flow Reynolds number approaches a critical value ($Re_D \approx 5 \times 10^5$) when the cylinder drag diminishes to levels as low as $C_D$ = 0.2 (Schewe, 1983). As the critical Reynolds number is reached, there are two discontinuities in the drag coefficient (Achenbach, 1968; Bearman 1969; and Schewe, 1983) that have been associated with the formation of *small, closed-recirculation bubbles on one or both sides of the cylinder* (Roshko & Fiszdon, 1969). When these recirculation bubbles are nominally symmetric on both sides of the cylinder, the diminution in drag is accompanied by azimuthal delay of boundary layer separation (up to $\theta \approx 147°$, Achenbach, 1968), a reduction in the width of the wake and the suppression of regular vortex shedding. Of course when the recirculation bubble occurs on one side of the cylinder, the reduction in drag is not as large but the flow asymmetry between the top and bottom surfaces results in the generation of lift ($C_L$ = O(1), Schewe, 1983). Similar asymmetries were also observed by Bearman (1969) and Shih et al. (1993).

A long-held notion has maintained that the onset of the drag crisis is associated with transition to turbulence. However, as noted by Roshko (1993), transition first occurs within the separating shear layer and its onset moves *upstream* as $Re_D$ increases. *It is remarkable that the lowest drag coefficient is attained at the critical Reynolds number when the boundary layer upstream of the closed recirculation bubble is laminar.* Furthermore, when transition occurs within the wall boundary layer at $Re_D > 5 \times 10^5$, the recirculation bubbles vanish, the separation point begins to move farther upstream and the drag increases (Roshko, 1961).

In a recent review article, Wygnanski (2004) conjectured that the effectiveness of the high-frequency actuation that is associated with virtual surface modification might be associated with transition to turbulence in the surface boundary layer. This issue was addressed in the earlier work of Glezer et al. (2003). In order to assess how transition to turbulence influences the effectiveness of the interaction domain between the jet and the cross flow, the flow over the surface of a 2-D cylinder was deliberately modified by tripping at $\theta = \pm 35^{o}$. Compared to the unforced flow, the azimuthal pressure distribution in the presence of the trip (Figure 6a) is similar to the pressure distribution at higher Reynolds numbers (Roshko & Fiszden, 1969) where the separation point of the tripped (but unforced) flow moves from $\theta = 85^{o}$ to $120^{o}$ as the cross-stream width of the wake decreases and the base pressure of the cylinder increases (accompanied by a decrease in pressure drag). When the jets are activated at $\gamma = 110^{o}$ (with the trips in place), there is a substantial decrease in the static pressure upstream and downstream of the actuators and as a result of the displacement of the streamlines of the external flow, the separation point moves to $\theta = 140^{o}$. The effect of the actuation on cross stream distributions of the Reynolds stresses *u'v'* in the presence of the trip is quite remarkable (Figure 6b, *x/D* = 3). While the Reynolds stress of the unforced flow is significantly higher than for the smooth cylinder, the actuation results in a Reynolds stress that is substantially *lower* (even lower than in the absence of the trip) as a result of enhanced small-scale dissipation.

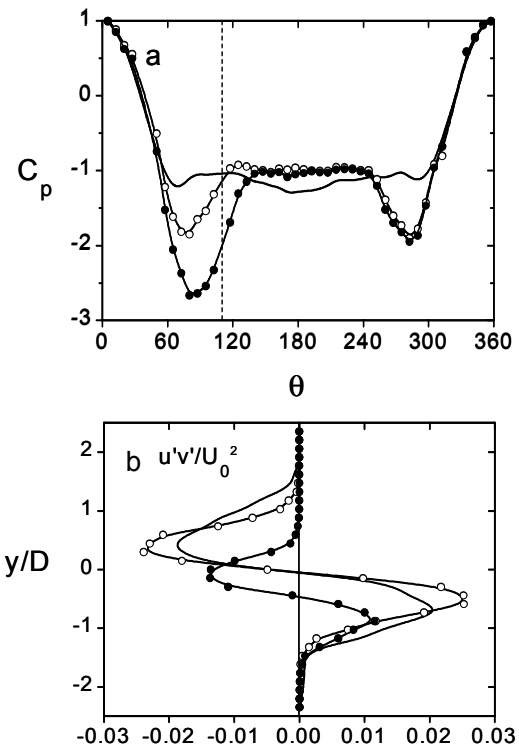


***Figure 6.*** *Azimuthal pressure distribution (a) and Reynolds stress (b) with boundary layer trip: unforced (○), forced (●), baseline (——).*

It is postulated that the role of the separation bubbles in creating the flow asymmetry that results in the increase in lift and concomitant reduction in drag near the critical Reynolds number is similar to the effects of the interaction domain between a jet actuator and the cross-flow (§ II.1). Furthermore, it appears that transition to turbulence plays a secondary role in the global effects on the flow and that the primary effect is the streamwise alteration of the pressure gradient by the local change in flow curvature that leads to changes in boundary layer evolution and downstream migration of separation.

## IV. Transient Aerodynamic Control

As discussed in §II above (see also Smith et al., 1998, Amitay and Glezer, 2002), actuation upstream of separation on stalled airfoil leads to flow reattachment and to the establishment of a higher (positive) lift force on the airfoil, which must be accompanied by a change in the vorticity flux and a net increase in circulation. The flow mechanisms which are associated with the onset

of flow separation and reattachment result in strong transient aerodynamic forces that can be exploited to further amplify the control authority of the actuation.

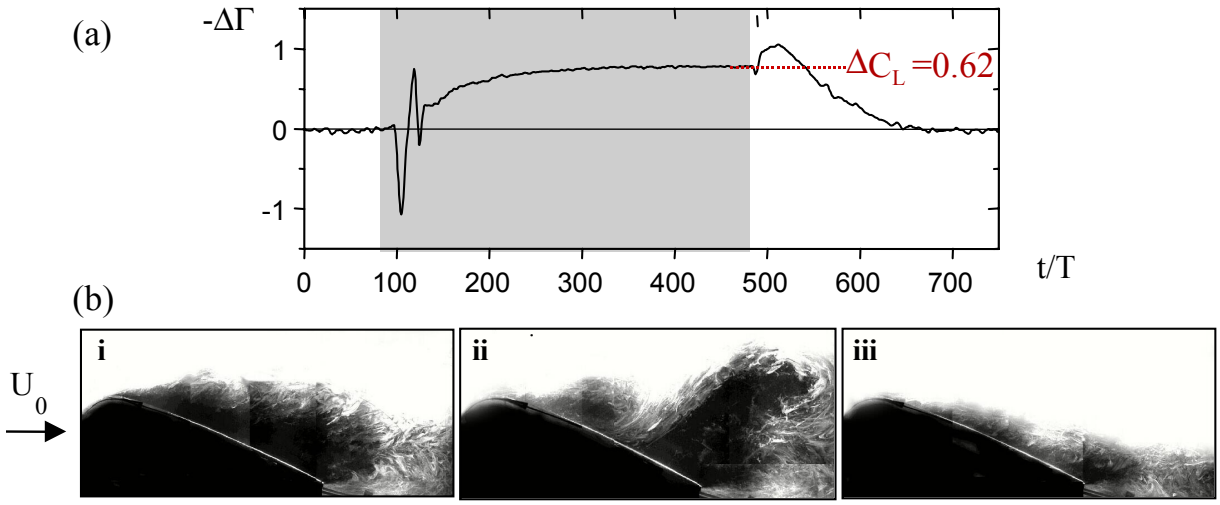


***Figure 7.*** *a) Time history of the circulation when control is activated, and b) Flow visualization images during flow reattachment: i. separated flow, ii. collapse of the separation domain, and iii. beginning of full reattachment*

For example, Figure 7a shows the time history of the incremental change in circulation (with respect to the unforced flow) about a stalled 2-D airfoil ($\alpha = 17.5^{o}$, $Re_C = 325{,}000$) during controlled reattachment and separation ($C_\mu = 1.8\text{x}10^{-3}$). These data show that the transition from separated to attached flow is accompanied by a transient, oscillatory change in the lift on time scale of O($100T_{act}$) before it ultimately converges to the time-averaged increment of 0.62 (relative to the stalled airfoil). The large changes in circulation indicate the organized shedding of vorticity concentration as shown in the corresponding flow visualization images in Figure 7b(i-iii) that are taken phase-locked to the control input. Note that the strong clockwise vortex following reattachment indicates *a reduction in lift* that is associated with the negative "trapped" vorticity that must shed off the airfoil. Immediately following the termination of the control and before the circulation decreases to the level of the separated flow, there is an increase in the (negative) circulation that is associated with *a momentary increase in lift* and appears to be similar to the variation of the circulation (and lift) during dynamic stall.

Earlier measurements at Georgia Tech (e.g., Amitay and Glezer, 2002) demonstrated that the flow transients that are induced by the removal or application of the control input can be exploited to improve the performance of the actuation at reduced levels of actuator momentum coefficient. The actuator resonance waveform (nominally at $F^+ = 10$) is pulse-modulated such that the period $t'$ and duty cycle $\hat{u}$ of the modulating pulse train are independently controlled. In what follows, the duty cycle is restricted to $\hat{u} = 0.25$ and the modulating frequency $f^+ = 1/t'$ is over a broad range. The variation of the phase-averaged circulation with $f^+$ is shown in Figures 8a-d for $f^+ = 0.27$, 1.1, 3.3 and 5.0, respectively.

The modulation frequency $f^+ = 0.27$ (Figure 8a), corresponds to the "natural" passage frequency of the vortices during the initial (transient) stages of the reattachment process (Figure III.2). The phase of each pulse of the modulating wave train is timed so that it re-triggers reattachment before the flow separates again. However, this phase is evidently a bit off, because the circulation apparently exhibits low-frequency variations (having a period of the order of 600T). When $f^+$ is increased to 1.1 the elapsed time between pulses within the modulating wave train is

decreased (Figure 8b) and the large oscillations in the circulation are substantially attenuated. This suggests that the modulating pulses are timed to prevent continuous shedding of large vortical structures and the corresponding variations in circulation. The recovery of an asymptotic circulation of ($\hat{\Gamma} \approx 0.45$) also suggests that the forcing allows the accumulation and maintenance of (clockwise) vorticity on the suction side of the airfoil even though the reattachment is unsteady and the circulation oscillates with peak-to-peak variations of 42% of its asymptotic mean level. Further increase in $f^+$ to 3.3 (Figure 8c) results in a circulation that is similar to the magnitude of the piecewise-averaged circulation in Figure 7b ($f^+ = 1.1$) but the absence of oscillations at the modulating frequency indicates optimal timing between the modulating pulses. It is remarkable that pulse modulation yields an increase of ~ 450% in the lift coefficient (when it reaches steady state) compared to continuous (quasi-steady) excitation *but at 25% of the jet momentum coefficient*. Finally, when the modulating frequency is increased further to $f^+ = 5$ (Figure 8d), the time between successive pulses of the modulating wave train is apparently too short to capture the unsteady vortical structures. The effectiveness of the modulation is minimal and the circulation returns to the same levels obtained with a continuous pulse train.

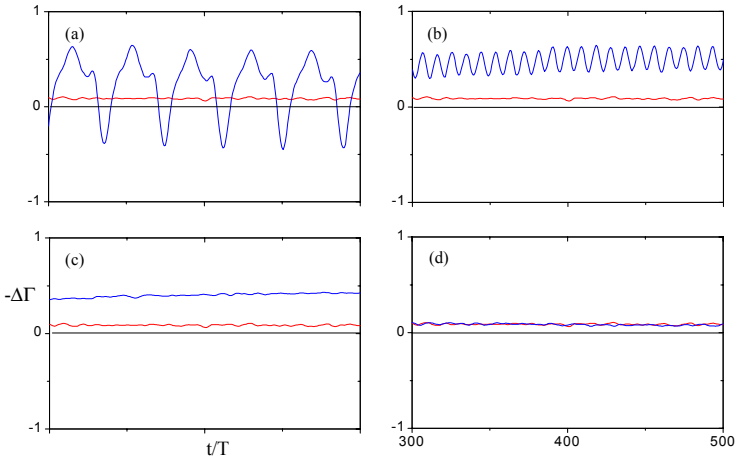


***Figure 8.*** *Phase-averaged circulation increment (blue trace) for $\alpha = 17.5^0$, $\gamma = 42^0$ and $f^+ = 0.27$(a), 1.1(b), 3.3(c), and 5.0(d). The red curve shows the circulation achieved by quasi steady forcing (no modulation).*

## V. Aerodynamic Control of Attached Flows using Trapped Vorticity

### *V.1 Controlled Trapped Vorticity*

The previous sections have discussed the utility of virtual shaping of the flow boundary for complete or partial suppression of separation using actuation that is effectively decoupled from the instabilities of the base flow. Because this approach to flow control does not rely on coupling to the global instabilities of the wake, it can be applied even in the absence of stall which is of particular interest for cruise conditions at low angles of attack when the baseline flow is fully attached. The recent work of Chatlynne et al. (2001) and Amitay et al. (2001) demonstrated the reduction of drag with minimal penalty in lift on a Clark-Y airfoil at low angles of attack for which the baseline flow is fully attached. This was achieved by the formation of a stationary recirculating flow domain next to the surface to alter the flow above the airfoil. This domain was formed by combining the activation of a high-frequency low-$C_\mu$ synthetic jet actuator that was placed downstream from a

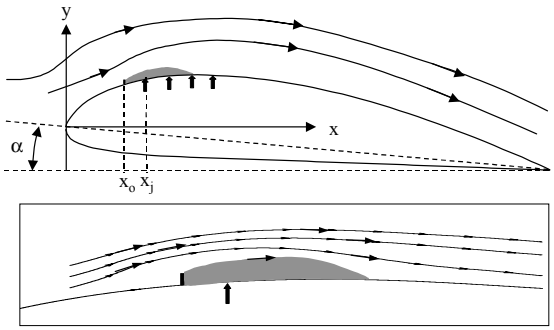


***Figure 9*** *Airfoil model showing an inset with the interaction domain between the jet and the cross flow.*

miniature surface-mounted passive obstruction that typically extended ~0.01*c* above the surface of the airfoil (Figure 9). The interaction between the synthetic jet and the obstruction resulted in increased suction in the vicinity of the actuator and a reduction in the magnitude of the pressure within the recovery domain towards the trailing edge. *These changes resulted in reductions in the pressure drag that were comparable to the magnitude of the pressure drag of the baseline configuration, and concomitantly in relatively small reductions (between nil and 8%) in lift.*

It is noteworthy that modification of the apparent aerodynamic shape of aero-surfaces in order to prescribe the streamwise pressure distribution and therefore to influence their aerodynamic performance was explored in a number of investigations in the 1940s and 50s. An example of this approach is the use of a stationary, mechanically trapped vortex to alter the apparent local surface curvature and therefore the direction of the external flow (Perkins and Hazen, 1953). It is clear that despite its attractive attributes, earlier implementations of virtual aerosurface shaping were limited by actuation technologies that included large-scale mechanical devices and blowing or suction at relatively large flow rates.

Scaling of the interaction domain when the jet is placed downstream of a miniature obstruction (Figure 9) were conducted by varying the actuation frequency. Time averaged PIV images of vorticity concentrations (and regularly-spaced cross stream velocity vectors) are shown in Figure 10a-d for $f_{act}$ = 139 Hz, 187 Hz, 362 Hz, and 850 Hz, respectively (the jet actuator is located immediately downstream of the obstruction). In the presence of actuation, the boundary layer separates downstream of the obstruction and a closed vortical recirculation domain is formed as a result of the jet actuation. The images show the clockwise (CW) spanwise vorticity concentration within the boundary layer and the ensuing separating shear layer, as well as the counter clockwise (CCW) vorticity near the surface downstream of the obstruction. The streamwise and cross stream extent of this domain are clearly influenced by the frequency (and by the strength of the jet).

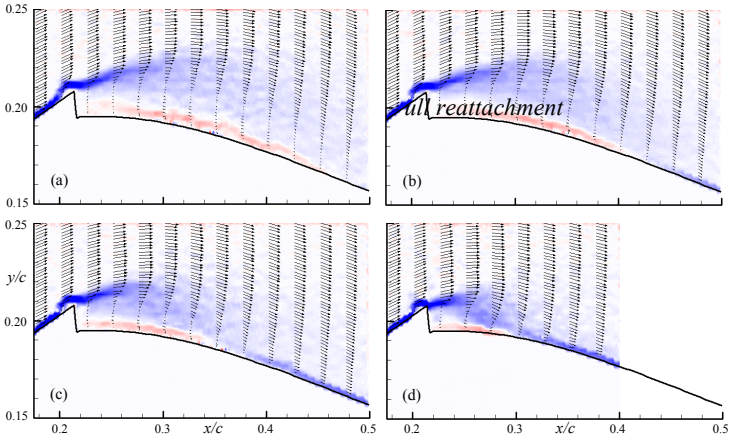


***Figure 10.*** *Time-averaged velocity vector and spanwise vorticity maps above the airfoil at $\alpha = 3^0$, $C_\mu = 1.2x10^{-3}$ and $Re_c$ = 381,000 for (a)*

The characteristic length of the interaction domain (or the trapped vortex) is determined (to first order) by the actuation wavelength $\lambda_{act}$. The circulation of this vortex is regulated on the cycle time of the actuation where vorticity from the upstream boundary layer is shed once per jet cycle following the suction stroke. Therefore, a "local" dimensionless frequency scale (e.g., Strouhal number, or $F^+$) that is based on the streamwise length scale of the trapped vortex (or the interaction domain) and the actuation frequency is nominally O(1) *regardless* of the scale of the trapped vortex relative to the chord of the airfoil. Because the scale of the interaction domain can vary between the full chord and less than 10% of the chord, it appears that unlike low-frequency separation control (i.e., forcing of the separated shear layer) which is characterized by

the advection and shedding of large scale vortices, a dimensionless frequency that scales with the streamwise length of the interaction domain may be inappropriate here.

### *V.2 Trapped Vortex Near the Trailing Edge: Manipulation of the Kutta Condition.*

Trapped vorticity concentrations near the trailing edge of an airfoil can be used for the manipulation of the Kutta condition near the trailing edge and thereby affect the entire circulation around the airfoil. This is accomplished by the use of a Gurney flap like device that is integrated with a synthetic jet. The Gurney flap is a flat plate that is typically mounted along the trailing edge of a conventional airfoil and normal to its lower (pressure) surface such that its height is nominally 1 to 2% of chord (as shown schematically in Figure 11). When the flap height is sufficiently small (less than 0.02*c*, Liebeck, 1978), it can lead to simultaneous increase in lift and reduction in drag presumably as a result from the displacement of a pair of small adjacent separation bubbles (essentially a counter-rotating vortex pair) that form along the upper and lower surfaces of the airfoil just upstream of its trailing edge (Figure 11a). The downwash associated with the increased lift in the presence of the Gurney flap apparently results in displacement and stretching of the separation bubbles (Figure 11b) and therefore in a smaller velocity deficit within the airfoil's wake. The measurements of Jeffrey et al. (2000) show how that a Gurney flap increases circulation over the airfoil by inducing the equivalent of a stationary vortex located near the trailing edge.

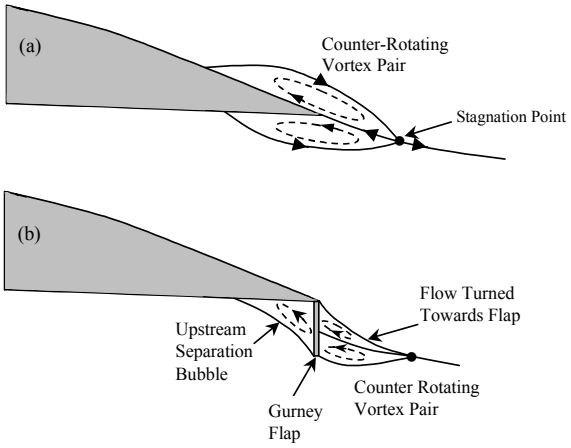


***Figure 11.*** *Conjectured flow structure near the trailing edge of an airfoil with a Gurney flap.*

Mandl (1959) used a split flap located on the pressure side of an airfoil combined with suction (at the flap) to trap a vortex and to enforce tangential flow near the trailing edges of the airfoil and the flap and alter the Kutta condition of the airfoil. The work of DeSalvo and Glezer (2002), has shown that the Kutta condition and thereby the global aerodynamic performance of a conventional airfoil at low angles of attack are manipulated by leveraging trapped vortices that are induced near the trailing edge by a miniature (0.016*c*) Gurney-like flap integrated with a synthetic jet actuator. These experiments use a modular NACA 4415 airfoil model having a chord measuring 461 mm (maximum thickness to chord ratio $t/c = 0.15$) which spans the entire 1 m x 1 m wind tunnel test section. A spanwise synthetic jet actuator driven by piezoelectric membranes (orifice measuring 140 x 0.5 mm) is integrated with a miniature flap having a characteristic height of 0.016and is movable along the pressure side surface of the airfoil. The airfoil is also instrumented with a circumferential array of 71 pressure ports (located at mid-span) and the velocity and vorticity fields in the cross-stream ($x$-$y$) plane, $z = 0$, above the airfoil (i.e., on the suction side) and in its wake are measured using particle image velocimetry (PIV). The experiments reported here are conducted at $Re_c = 460{,}000$ (based on the free stream velocity and the chord of the airfoil).

The addition of a Gurney flap that scales on the order of a few percent of the chord length of a conventional airfoil can lead to an increase in lift that may be accompanied by an increase or

decrease in pressure drag. The aerodynamic characteristics of the present hybrid actuator are compared with a "conventional" 0.014*c* surface-normal Gurney flap when both are mounted flush with the trailing edge of the baseline (smooth) airfoil. Figures 12a and b show the variations with angle of attack ($-4^o < \alpha < 8^o$) of the lift and (pressure) drag coefficients ($C_L$ and $C_{Dp}$) and the corresponding pressure drag polar for the baseline (smooth) airfoil, and for the airfoil combined with the conventional Gurney flap and with the jet integrated hybrid actuator. The addition of a conventional Gurney flap leads to an increase in the lift coefficient (nominally 0.12) that is almost invariant over the entire range of angles of attack tested here and to an increase in pressure drag (from 112% at $\alpha = 0^o$ to 46% at $\alpha = 8^o$). The data in Figure 12 show that the aerodynamic characteristics of the baseline airfoil combined with the hybrid actuator are reasonably similar to what is measured with the conventional Gurney flap.

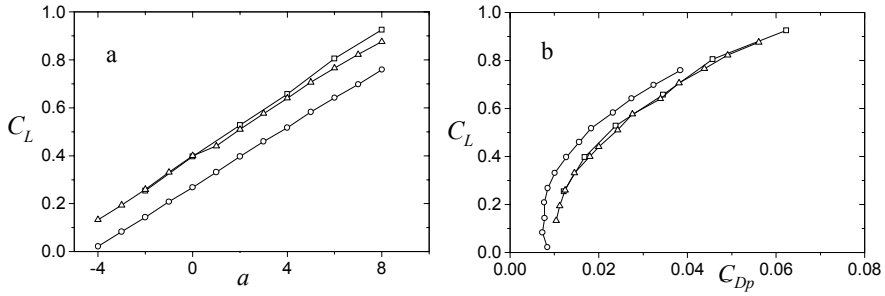


***Figure 12*** *The variations of $C_L$ with a (a),and the pressure drag polar (b). (○) Smooth, (Δ) Gurney flap and (□) hybrid actuator.*

The effect of the actuation on the aerodynamics of the airfoil for angles of attack within the range $-2^o < \alpha < 8^o$ is shown in Figure 13. Although in the absence of actuation the addition of the hybrid actuator (at $x_G/c = 0.94$) results in an increase in lift, it is accompanied by an increase in pressure drag that leads to an overall decrease in $L/D_p$ compared to the baseline (smooth) airfoil. When actuation is applied ($C_\mu = 8 \cdot 10^{-3}$), there is a substantial increase in $L/D_p$ (Figure 13a) compared to both the baseline airfoil and and the airfoil with inactive hybrid actuator over the entire range of angles of attack. At this streamwise position of the actuator, the maximum lift to pressure drag ratio is obtained at $\alpha = 0^o$ ($L/D_p = 36.3$), which is an increase of 45% over the airfoil with the inactive actuator, but more significantly an increase of more than 15% relative to the smooth airfoil. The corresponding pressure drag polar (Figure 13b) shows that for a given lift coefficient, there is a decrease in the pressure drag compared to both the inactive actuator and smooth airfoils. As $C_L$ increases, the decrement in pressure drag increases relative to the smooth airfoil and decreases relative to the unactuated airfoil.

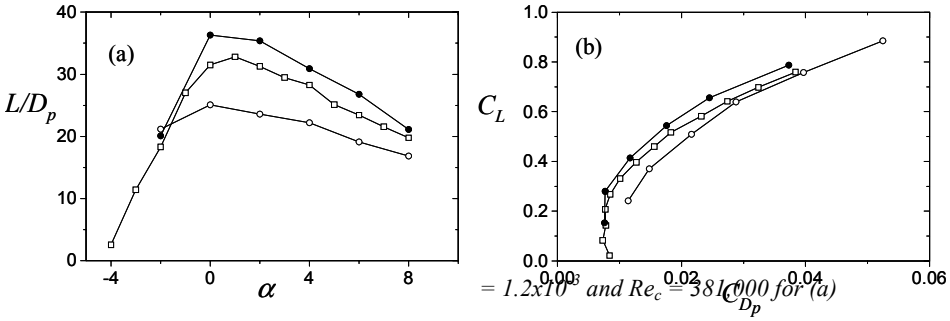


*ull reattachment*

*= 1.2x10⁶ and $Re_c$ = 381,000 for (a)*

***Figure 13*** *(a) Variation of $L/D_p$ with $\alpha$, and (b) the pressure drag polar: (□) Smooth, (○) inactive (●) and active hybrid actuator.*

The effectiveness of the actuation can be continuously varied by adjusting the strength of the control jet as measured by its momentum coefficient $C_\mu$. Figure 14 shows the variation with $C_\mu$

of the normalized increments (relative to the baseline airfoil) of lift to drag ratio, at $\alpha = 0^o$. For the unactuated flap (i.e., $C_\mu = 0$), the respective increases in lift and drag are 35% and 68%, and the corresponding decrease in $L/D_p$ is 20%. As $C_\mu$ is increased, there is a monotonic decrease in both the normalized lift and pressure drag and an increase in $L/D_p$. The lift to pressure drag ratio of the baseline airfoil is attained at $C_\mu = 4.9 \cdot 10^{-3}$ when the lift and drag coefficients are each 8% larger than for the baseline airfoil. At the highest actuation level that was achieved with the present actuators ($C_\mu = 8 \cdot 10^{-3}$), $L/D_p$ increases by 19%, the pressure drag decreases by 16% while the lift is nominally unchanged.

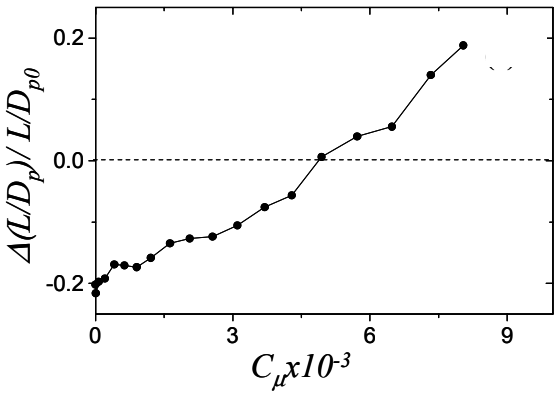


***Figure 14*** *Variation with $C_\mu$ of the normalized increments of the lift to drag ratio for $\alpha = 0^o$.*

These data show that the aerodynamic performance of a conventional airfoil can be continuously varied by adding a small flap integrated with a fluidic actuator. *In fact, it is remarkable that the aerodynamic performance of the airfoil can be varied from a configuration that is essentially an airfoil with a conventional Gurney flap through an airfoil that has similar performance as that of the smooth (baseline) airfoil to an airfoil that has higher lift to pressure drag ratio.*

## V. Concluding Remarks

Recent work on a novel approach to the control of the aerodynamic performance of lifting surfaces by *fluidic modification of their apparent aerodynamic shape, or virtual aerosurface shaping* is reviewed. This flow control approach emphasizes fluidic modification of the "apparent" aerodynamic shape of the surface with the objective of altering or prescribing the local streamwise pressure gradient. The actuation is typically effected by forming a controlled interaction domain between a surface-mounted fluidic actuator (e.g., a synthetic jet) and the cross flow above the surface. An important ingredient of virtual aerosurface shaping is that the characteristic wavelength of the actuation is at least an order of magnitude smaller than the relevant local or global length scale in the flow so that the interaction between the actuator and the cross flow (e.g., upstream of separation) is essentially time-invariant on the global time scale of the flow and therefore global effects (e.g., vorticity shedding) are effectively *decoupled* from the actuation frequency. In contrast, conventional aerodynamic flow control schemes have typically focused on the mitigation of separation and stall near the leading edge or on flaps by relying on global manipulation of the *coupled* instability of the separating shear layer and the wake such that the characteristic actuation period scales with the advection time of the affected flow domain.

The present paper reviews the applications of virtual aerosurface shaping in two domains of the flight envelope. The first is at post stall angles of attack where the ability to suppress separation implies robust control over large changes in circulation and accumulation and shedding of vorticity. The second domain is that of small angles of attack when the baseline flow is typically fully attached and therefore less amenable to flow control approaches that require separation.

Earlier work at Georgia Tech demonstrated the utility of high-frequency actuation for virtual surface shaping for the suppression of flow separation at post-stall angles of attack. As noted

above, an important attribute of this approach is that the actuation is inherently decoupled from the instability of the wake and therefore separation can be either completely (or partially) suppressed without the formation and shedding of large coherent vortical structures into the wake and time-dependent changes in circulation that can lead to unsteady aerodynamic forces. That the actuation is not restricted to narrow band receptivity at the unstable frequencies of the base flow enables a broader control bandwidth that is essentially limited by the response of the actuator. Furthermore, this broader control bandwidth can also be used to augment the quasi-steady aerodynamic forces by exploiting the dynamics of a locally separated flow domain using a temporally-modulated actuation to control the rate of vorticity shedding into the wake and concomitantly changes in circulation that accompany the inception and termination of stall. Virtual surface shaping may be used to keep a controlled trapped vortex over the airfoil thus achieving an increase in lift that may be similar to what has been observed in dynamic stall.

In addition to controlling separated flows, alteration of the apparent aerodynamic shape of airfoils offers unique control opportunities at low angles of attack *when the baseline flow is fully attached*. Work in this area demonstrated reduction in drag with minimal penalty in lift at low angles of attack by the formation of a stationary recirculating flow domain next to the surface near the leading or trailing edges. This domain is formed by combining a synthetic jet actuator placed downstream of a miniature O(0.01*c*) surface-mounted passive obstruction. The reduction in pressure drag was comparable to the magnitude of the pressure drag of the baseline configuration. A synthetic jet combined with a miniature O(0.016*c*) Gurney flap was used to manipulate the Kutta condition near the trailing edge of an airfoil and it was shown that by simply controlling the strength (momentum coefficient) of the jet actuator, the aerodynamic characteristics of the airfoil can be *continuously* varied from a configuration that has a Gurney flap to that of the (baseline (smooth) airfoil to an airfoil that has higher lift to drag ratio than the baseline.

### Acknowledgement

The research work at Georgia Tech was supported in major part by grants from the Air Force Office of Scientific Research (AFOSR). Additional support was provided by The Boeing Company and the Georgia Institute of Technology.

## References

Achenbach E., Distribution of local pressure and skin friction around a circular cylinder in cross flow up to Re=5 x $10^5$, *J. Fluid Mech*., **34**, pp. 625-639, 1968.

Ahuja, K. K. and Burrin, R. H., Control of flow separation by sound. AIAA Paper 84-2298, 9th AIAA/NASA Aeroacoustics Conference, Williamsburg, VA., 1984.

Amitay, M., Honohan, A., Trautman, M. and Glezer, A. Modification of the aerodynamic characteristics of bluff bodies using fluidic actuators, AIAA Paper 97-2004, 1997.

Amitay, M., Smith, B. L. and Glezer, A., Aerodynamic Flow Control using Synthetic Jet Technology, AIAA Paper 98-0208, 1998.

Amitay, M. and Glezer, A., Aerodynamic flow control of a thick airfoil using synthetic jet actuators, Proc. of the 3rd ASME/JSME Joint Fluids Engineering Conference, 1999.

Amitay, M., Kibens, V., Parekh, D. E. and Glezer, A., Flow Reattachment Dynamics over a Thick Airfoil Controlled by Synthetic Jet Actuators, AIAA Paper 99-1001, 1999.

Amitay, M., Pitt, D., Kibens, V., Parekh, D. and Glezer, A., Control of Internal Flow Separation using Synthetic Jet Actuators, AIAA 2000-0903, 2000.

Amitay, M., Smith, D. R., Kibens, V., Parekh, D. and Glezer A., Aerodynamic Flow Control over an Unconventional Airfoil using Synthetic Jet Actuators, *AIAA Journal*, **39**, 2001.

Amitay, M., Horvath, M., Michaux, M. and Glezer, A., Virtual Aerodynamic Shape Modification at Low Angles of Attack using Synthetic Jet Actuators, AIAA Paper 2975, 2001.

Amitay, M., Smith, D.R., Kibens, V., Parekh, D.E. and Glezer, A., Modification of the Aerodynamics Characteristics of an Unconventional Airfoil Using Synthetic Jet Actuators, *AIAA Journal*, **39**, 361-370, 2001.

Amitay, M. and Glezer, A., Controlled Transients of Flow Reattachment over Stalled Airfoils, *International Journal of Heat Transfer and Fluid Flow,* **23***,* 690-699, 2002.

Bearman, P.W., On vortex shedding from a circular cylinder in the critical Reynolds number regime, *J. Fluid Mech*., **37**, pp. 577-585, 1969.

Chang R. C., Hsiao F. B. and Shyu R. N., "Forcing Level Effects of Internal Acoustic Excitation on the Improvement of Airfoil Performance", *Journal of Aircraft*, **29**, 1992.

Chatlynne, E., Rumigny, N., Amitay, M. and Glezer, A., Virtual Aero-Shaping of a Clark-Y Airfoil using Synthetic Jet Actuators, AIAA Paper 2001-0732, 2001

DeSalvo, M. Amitay, M. and Glezer, A., Modification of the Aerodynamic Performance of Airfoils at Low Angles of Attack: Trailing Edge Trapped Vortices, AIAA Paper 2002-3165, 2002.

Erk, P. P., Separation Control on a Post-Stall Airfoil Using Acoustically Generated Perturbations. Ph.D. Dissertation, Technische Universitat Berlin, Germany, 1997.

Fung, P. and Amitay, M., "Active Flow Control Application on a Mini Ducted Fan UAV", *Journal of Aircraft*, **39**, 561-571, 2002.

Glezer, A. and Amitay, M. "Synthetic Jets," *Ann. Rev. Fluid Mech*, **24**, 2002

Glezer, A., Amitay, M. and Honohan, A., "Aspects of Low- and High-Frequency Aerodynamic Flow Control", AIAA paper 2003-0533, 2003.

Honohan, A. M., Amitay, M. and Glezer, A., "Aerodynamic Control using Synthetic Jets", AIAA-paper 2000-2401, Fluids 2000 Conference, Denver, CO, 2000.

Honohan, A. M., "The Interaction of Synthetic Jets with Cross Flow and the Modification of Aerodynamic Surfaces," Ph.D. Dissertation, Georgia Institute of Technology, Atlanta, GA, 2003.

Jeffrey, D., Zhang, X. and Hurst, D., Aerodynamics of Gurney Flaps on a Single-Element High-Lift Wing, *Journal of Aircraft 37*(2), pp. 295-301, 2000.

Kondor, S., Amitay, M., Parekh, D., Fung, P. and Glezer, A., "Active Flow Control Application on a Mini Ducted Fan UAV", AIAA paper 2001-2440, 2001.

Liebeck, R.H.. Design of Subsonic Airfoils for High Lift, *Journal of Aircraft,* **15**, pp. 547-561, 1978.

Mandl, P., Effect of Standing Vortex on Flow about suction aerofoils with Split Flaps, *Nat. Res. Council of Canada, Aero. Rep. No*. 234, 1959.

Neuberger D. and Wygnanski I., "The Use of a Vibrating Ribbon to Delay Separation on Two Dimensional Airfoils", Proceedings of Air Force Academy Workshop in Unsteady Separated

Flow (Colorado Springs, CO), edited by F.J Seiler, Research Lab Report TR-88-0004, U.S. Air Force Academy, 1987

Pal D. and Sinha K., Controlling an Unsteady Separating Boundary Layer on a Cylinder with an active Compliant Wall, AIAA Paper 97-0212, 35th Aerospace Sciences meeting, Reno, NV, 1997.

Pack Melton, L., Yao, C.-S., and Seifert, A. "Application of Excitation from Multiple Locations on a Simplified High-Lift System," AIAA Paper 2324, 2004.

Perkins, C.D. and Hazen, D., Some recent advances in Boundary Layer and Circulation Control, Fourth Anglo-American Aeronautical Conference, 1953.

Roshko A, Experiments on the flow past a circular cylinder at very high Reynolds number, *J. Fluid Mech*., **10**, pp. 345-356, 1961.

Roshko A., Perspectives on bluff body aerodynamics, *Journal of Wind Engineering and Industrial Aerodynamics*, **49**, pp. 79-100, 1993.

Roshko A. and Fiszdon W., On the persistence of transition in the near wake, *Problems of Hydrodynamics and Continuum Mechanics*. Soc. Industrial and Appl. Math., Philadelphia, pp. 606-616, 1969.

Schewe G., On the force fluctuations acting on a circular cylinder in a cross flow from sub-critical to trans-critical Reynolds numbers, *J. Fluid Mech*., **133**, pp. 265-285, 1983

Seifert, A., Bachar, T., Koss, D., Shepshelovich, M. & Wygnanski, I. Oscillatory blowing: a tool to delay boundary-layer separation. *AIAA Journal***. 31,** 2052-2060, 1993.

Seifert, A., Darabi, A. and Wygnanski, I., Delay of airfoil stall by periodic excitation, *J. Aircraft 33*(4), pp. 691-698, 1996.

Smith, B. L. and Glezer, A., The Formation and Evolution of Synthetic Jets, Physics of Fluids, Vol. 10, No. 9, 1998.

Smith, D. R., Amitay, M., Kibens, V., Parekh, D. and Glezer, A., Modification of lifting body aerodynamics using synthetic jet actuators, AIAA Paper 98-0209, 1998.

Smith, B. L. and Glezer, A., "Jet Vectoring using Synthetic Jets," *J. Fluid Mech*., **458**, 1-34, 2002.

Williams, D., Acharya, M., Bernhardt, K. & Yang, L., The Mechanism of Flow Control on a Cylinder with the Unsteady Bleed Technique, AIAA Paper, 29 th Aerospace Sciences meeting, Reno, NV, 1991.

Wiltse, J. M. and Glezer, A., Direct excitation of Small-Scale Motions in Free Shear Flows, *Physics of Fluids*, **10**, 2026-2036, 1998.

Wu, J. –Z., Lu, X.-Y., Denny, A. G., Fan, M., and Wu, J.-M., "Post Stall Flow Control on an Airfoil by Local Unsteady Forcing," *J. Fluid Mech.*, **371**, 21-58, 1998.

Wygnanski, I., "The Variables Affecting the Control of Separation by Periodic Excitation," AIAA Paper 2004-2505, 2004.

AVT-111 Specialists' Meeting on Enhancement of NATO Military Flight Vehicle Performance by Management of Interacting Boundary Layer Transition and Separation

DISCUSSION

1. REFERENCE No. OF THE PAPER: 1
2. DISCUSSOR´S NAME: Wagner
3. AUTHOR´S NAME: Glezer

QUESTION:

1. Is the boundary layer actually laminar?
2. At low angles of attack, $\alpha$, you got a reduction of pressure drag by actuation. What happens with the viscous drag?

AUTHOR´S REPLY

1. Yes. Heat flux gage data (AIAA J. May 2003) confirm this, over a large portion of the upper surface.
2. We speculate that the reduction in overall wake width should also decrease the viscous drag. Perhaps it could be quantified with phase averaged wake surveys – a very time consuming effort. Susceptible to measurement technique limitations.